



Signal-dependent regulation of the sea urchin skeletogenic gene regulatory network



Zhongling Sun, Charles A. Etensohn*

Department of Biological Sciences, Carnegie Mellon University, 4400 Fifth Avenue, Pittsburgh, PA 15213, USA

ARTICLE INFO

Article history:

Received 16 June 2014

Received in revised form 7 October 2014

Accepted 8 October 2014

Available online 16 October 2014

Keywords:

Gene regulatory network

Morphogenesis

Skeleton

Biomineralization

Sea urchin

Primary mesenchyme cells

ABSTRACT

The endoskeleton of the sea urchin embryo is produced by primary mesenchyme cells (PMCs). Maternal inputs activate a complex gene regulatory network (GRN) in the PMC lineage in a cell-autonomous fashion during early development, initially creating a uniform population of prospective skeleton-forming cells. Previous studies showed that at post-blastula stages of development, several effector genes in the network exhibit non-uniform patterns of expression, suggesting that their regulation becomes subject to local, extrinsic cues. Other studies have identified the VEGF and MAPK pathways as regulators of PMC migration, gene expression, and biomineralization. In this study, we used whole mount *in situ* hybridization (WMISH) to examine the spatial expression patterns of 39 PMC-specific/enriched mRNAs in *Strongylocentrotus purpuratus* embryos at the late gastrula, early prism and pluteus stages. We found that all 39 mRNAs (including several regulatory genes) showed non-uniform patterns of expression within the PMC syncytium, revealing a global shift in the regulation of the skeletogenic GRN from a cell-autonomous to a signal-dependent mode. In general, localized regions of elevated gene expression corresponded to sites of rapid biomineral deposition. We used a VEGFR inhibitor (axitinib) and a MEK inhibitor (U0126) to show that VEGF signaling and the MAPK pathway are essential for maintaining high levels of gene expression in PMCs at the tips of rods that extend from the ventral region of the embryo. These inhibitors affected gene expression in the PMCs in similar ways, suggesting that VEGF acts via the MAPK pathway. In contrast, axitinib and U0126 did not affect the localized expression of genes in PMCs at the tips of the body rods, which form on the dorsal side of the embryo. Our results therefore indicate that multiple signaling pathways regulate the skeletogenic GRN during late stages of embryogenesis—VEGF/MAPK signaling on the ventral side and a separate, unidentified pathway on the dorsal side. These two signaling pathways appear to be activated sequentially (ventral followed by dorsal) and many effector genes are subject to regulation by both pathways.

© 2014 Elsevier B.V. All rights reserved.

The primary mesenchyme cells (PMCs) of the sea urchin embryo, which produce the embryonic and early larval skeleton, are a model system for studying specification, differentiation, and morphogenesis (Etensohn, 2013; McIntyre et al., 2014; Wilt and Etensohn, 2007). PMCs are the sole descendants of the four large micromeres, which arise at the vegetal pole of the embryo during cleavage. At the mesenchyme blastula stage, the large micromere progeny undergo an epithelial–mesenchymal transition (EMT) and ingress into the blastocoel, after which they are referred to as PMCs (Wilt and Etensohn, 2007). After EMT, PMCs migrate along the blastocoel wall and arrange themselves in a characteristic, subequatorial ring pattern. The PMC ring consists of two clusters of cells (the ventrolateral clusters, or VLCs) that are connected by two cellular chains

– a short ventral chain and a long dorsal chain. Late in gastrulation, a few PMCs from each VLC migrate toward the animal pole; these PMCs constitute the longitudinal chains (Fig. 1). As the PMCs migrate, their filopodia fuse, forming a cable-like structure that links the cells in a single, syncytial network (Hodor and Etensohn, 1998). Despite the fact that the PMCs are joined in a syncytium, the exchange of gene products between cells is quite limited, and mRNAs and proteins are largely confined to the PMCs in which they are produced (Guss and Etensohn, 1997; Harkey et al., 1992; Illies et al., 2002; Lapraz et al., 2009; Livingston et al., 2006; Urry et al., 2000; Wilt et al., 2008).

The arrangement of the PMCs during gastrulation prefigures the morphology of the skeleton. Skeletogenesis begins with the formation of one triradiate spicule rudiment in each VLC at the mid-gastrula stage. These two skeletal rudiments subsequently elongate and branch to form the two spicules of the skeleton, which exhibit mirror-image symmetry. The PMCs in the dorsal chain produce the body rods and those in the ventral chain form the ventral transverse rods. The PMCs in the longitudinal chains give rise to the

* Corresponding author. Department of Biological Sciences, Carnegie Mellon University, 4400 Fifth Avenue, Pittsburgh, PA 15213, USA. Tel.: +1 412 268 5849; fax: +1 412 268 7129.

E-mail address: ettensohn@cmu.edu (C.A. Etensohn).

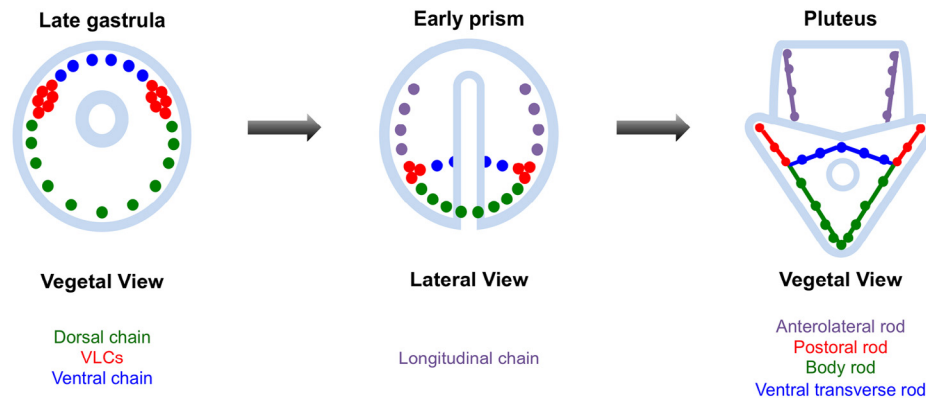


Fig. 1. Schematic diagrams of PMC patterning and skeletogenesis in *S. purpuratus* at the late gastrula, early prism and pluteus stage. PMCs are color-coded to indicate their position within the syncytial network and the specific skeletal rods that they produce. VLC = ventrolateral cluster.

dorsoventral connecting rods, which in *Strongylocentrotus purpuratus* curve ventrally, forming the anterolateral rods (Fig. 1). In many other species, the dorsoventral connecting rods branch to form the anterolateral and recurrent rods. During late stages of embryogenesis, the body rods, anterolateral rods, and postoral rods elongate rapidly through the addition of new biomineral at their tips, while the ventral transverse rods cease their growth (Etensohn and Malinda, 1993; Guss and Etensohn, 1997).

The intricate and reproducible pattern of the embryonic skeleton is regulated by interactions between PMCs and neighboring cells. Isolated micromeres cultured in plain seawater fail to produce spicules unless horse serum is added (Okazaki, 1975). Hardin et al. (1992) and Armstrong et al. (1993) showed that the induction of supernumerary triradiate spicule rudiments by NiCl_2 is a consequence of a ventralization of the ectoderm. Furthermore, Etensohn and Malinda (1993) showed that photoablation of a patch of ectodermal cells at the tip of the postoral arm inhibits the elongation of the underlying postoral rod, suggesting that short-range, ectoderm-derived cues are required for rod elongation. The stereotypical pattern of elongation rates of the various skeletal rods observed *in vivo* also supports the view that local cues regulate skeletal growth (Guss and Etensohn, 1997).

Vascular endothelial growth factor-3 (VEGF3) has recently been shown to play an important role in PMC migration, gene expression and biomineralization (Adomako-Ankomah and Etensohn, 2013; Duloquin et al., 2007; Knapp et al., 2012). Whole mount *in situ* hybridization (WMISH) reveals that *vegf3* is expressed selectively by ectoderm cells that overlie sites of rapid skeletal growth (Adomako-Ankomah and Etensohn, 2013; Duloquin et al., 2007). The localized pattern of *vegf3* expression is controlled by a complex cascade of signaling molecules and gene regulatory interactions that pattern the ectoderm (Li et al., 2013, 2014; McIntyre et al., 2013; Molina et al., 2013). Treatment of embryos with U0126, a MEK inhibitor, or axitinib, a VEGFR inhibitor, at late developmental stages results in an inhibition of biomineral deposition and the formation of truncated skeletal rods (Adomako-Ankomah and Etensohn, 2013; Sun and Etensohn, unpublished observations). Because receptor tyrosine kinases often signal via the MAPK cascade (Schlessinger, 2000), these observations suggest that VEGF3 regulates skeletal growth through this pathway.

A complex gene regulatory network (GRN) is deployed in the large micromere-PMC lineage (Oliveri et al., 2008; Rafiq et al., 2012, 2014). The PMC GRN is activated by polarized, maternal inputs and requires the unequal cleavage of vegetal blastomeres (Sharma and Etensohn, 2010). These inputs entrain the cell-autonomous deployment of many downstream genes in the network, including many terminal effector genes (Etensohn, 2013; Oliveri et al., 2008;

Rafiq et al., 2012, 2014). The MAPK pathway is selectively activated in the large micromere-PMC lineage during early development, probably by cell-autonomous mechanisms, and this pathway plays an essential role in the deployment of the network (Fernandez-Serra et al., 2004; Rafiq et al., 2014; Röttinger et al., 2004).

The developmental consequences of the cell-autonomous phase of PMC differentiation are evident from the development of micromeres that have been cultured in seawater without serum or other supplements. Under such conditions, micromeres divide and their descendants undergo striking changes in behavior, becoming migratory and fusogenic (Hodor and Etensohn, 1998; McCarthy and Spiegel, 1983; Okazaki, 1975), but they do not form spicules. It seems likely that this early, cell autonomous phase of GRN deployment is responsible for the activation of many effector genes that show maximal levels of expression at the blastula stage, prior to PMC ingression (Rafiq et al., 2014). At least two downstream effectors, *sm50* and *msp130*, are expressed at similar levels in the presence or absence of serum (Page and Benson, 1992). In addition, *sm50* is expressed at high levels even when early embryos are dissociated and the cells cultured under conditions that minimize cell-cell contacts (Stephens et al., 1989). Based on qualitative WMISH studies, the initial, cell-autonomous phase of GRN deployment appears to produce a relatively homogeneous population of cells; i.e., effector genes are expressed relatively uniformly among PMCs at the late blastula stage (Rafiq et al., 2012, 2014). Later in development, however, several effector mRNAs show non-uniform distributions within the PMC syncytium, suggesting that local signals regulate the expression of the cognate genes (Adomako-Ankomah and Etensohn, 2011; Cheers and Etensohn, 2005; Guss and Etensohn, 1997; Harkey et al., 1992; Illies et al., 2002; Livingston et al., 2006).

To gain a better understanding of the regulation of skeletal morphogenesis by ectodermal cues, we analyzed and classified the spatial expression patterns of 39 PMC-enriched transcripts in *S. purpuratus* embryos at three late (post-blastula) stages of embryogenesis. We report that: 1) many genes in the skeletogenic GRN, including both regulatory genes and effector genes, show non-uniform patterns of expression within the PMC syncytium at late developmental stages, reflecting the influence of local, ectoderm-derived cues; 2) the effect of these local cues is to *maintain* the expression of effector genes that are initially activated by cell-autonomous mechanisms but decline in expression except in those regions where appropriate signals are provided; 3) the PMC syncytium consists of distinct sub-populations of PMCs with different molecular properties; 4) regions of elevated gene expression generally correspond to sites of skeletal rod growth; 5) multiple ectodermal signals regulate gene expression and skeletal growth. One of these cues, VEGF3, regulates gene expression and skeletal rod selectively on the ventral side

of the embryo. Our findings support the view that the skeletogenic GRN undergoes a global shift in its regulation from a cell-autonomous to a signal-dependent mode, resulting in distinctive molecular properties of subpopulations of PMCs within the syncytial network that, in turn, influence local patterns of skeletal growth and morphology.

1. Results

1.1. Mapping the spatial expression patterns of PMC-specific/enriched transcripts at the late gastrula, early prism and pluteus stages

To explore the regulation of PMC gene expression by ectoderm-derived cues, we examined the spatial expression patterns of 39 PMC-specific/enriched mRNAs in *S. purpuratus* embryos at the late gastrula, early prism, and pluteus stages (32, 48, and 76 hpf, respectively). The accession numbers associated with these genes are shown in Table 1. Among these genes, 19 encoded transmembrane or secreted proteins that function in biomineralization (*can1*, *Clectin*, *msp130*, *msp130rel1*, *msp130rel2*, *msp130rel3*, *otop2L*, *p16*, *p16rel1*, *p16rel2*, *p19*, *p58A*, *sm20*, *sm27*, *sm29*, *sm30A*, *sm37*, *sm49*, and *sm50*) and three encoded transcription factors (*alx1*, *ets1*, and *jun*). The precise developmental functions of the remaining proteins have not been determined; these proteins included five transmembrane proteins [*aqp9*, *kirrelL*, *net7*, *SPU_027993*, and *Ig/TM* (the same protein referred to as “Scaffold17:88148–92454” by

Rafiq et al., 2014)], three metalloproteases (*cbpdEL*, *mt1–4*, and *mt5*), three secreted proteins (*frp*, *p41*, and *p133*), two cellular enzymes (*pks2* and *sfk3*), and four other cytoplasmic proteins (*ank*, *casc1*, *cp*, and *gabrb3L*).

The expression patterns of these mRNAs were classified into 4–5 categories at each developmental stage, based primarily on the site(s) of maximal expression (Fig. 2). To categorize gene expression patterns, all the genes expressed at a given stage were grouped into synexpression classes and numbered based on the number of genes contained in the class; e.g., the class with the most gene members was designated Class 1, the class with the next most members was designated Class 2, and so on. This classification was carried out independently for developmental stage (i.e., there is no direct correspondence between Class 1 at the late gastrula stage and Class 1 at the prism stage). We adopted this scheme because no synexpression class remained strictly coherent through time.

At the late gastrula stage, the expression of 38 genes was detectable by WMISH and five expression categories were identified based on the sites of maximal expression within the subequatorial PMC ring. 19 genes were expressed maximally in the VLCs (Fig. 3, Class I), nine genes were expressed at the highest level in the VLCs and the ventral chain (Fig. 2, Class II), five genes were expressed at the highest level in the VLCs and the dorsal chain (Fig. 3, Class III); four genes were uniformly expressed in all PMCs (Fig. 3, Class IV); and one gene (*pks2*) was expressed only in the ventral chain (Fig. 3, Class V; see Beeble and Calestani, 2012). In some cases, genes with similar functions exhibited distinct expression patterns. For example,

Table 1
SPU IDs, Genbank accession numbers and WMISH conditions of genes examined.

Gene Name	SPU ID	GENBANK Accession Number	Temperature (°C)	Concentration (ng/μl)
<i>alx1</i>	SPU_022817/025302	AY277399	55	1
<i>ank</i> (<i>ank2h/ank3_1/Hypp_3119</i>)	SPU_000908/021014	DN805441	55	1
<i>aqp9</i>	SPU_004511	DN581355	55	1
<i>can1</i>	SPU_012518	DN576288	55	1
<i>casc1</i>	SPU_022570	DN789104	55	2
<i>cbpdEL</i>	SPU_007682	DN579627	60	2
<i>Clectin</i>	SPU_007882	DN578017	55	2
<i>cp</i>	SPU_027885	DN585351	55	1
<i>ets1/2</i>	SPU_002874	DN562391	55	1
<i>frp</i>	SPU_022598	DN580870	55	1
<i>gabrb3L</i>	SPU_007767	DN805603	55	1
<i>Ig/TM</i>	N/A	DN791856	55	2
<i>jun</i>	SPU_003102	DN781891	60	1
<i>kirrelL</i>	SPU_024995	DN578096	55	2
<i>msp130</i>	SPU_002088/013821	DN805022	55	0.5
<i>msp130rel1</i>	SPU_013822	DN581882	55	2
<i>msp130rel2</i>	SPU_016506	DN783962	55	1
<i>msp130rel3</i>	SPU_013823	BG786515	50	2
<i>mt1–4</i>	SPU_013670	DN582135	55	1
<i>mt5</i>	SPU_028749	DN580804	60	2
<i>net7</i>	SPU_025068	DN561474	55	1
<i>otop2L</i>	SPU_004767	DN787409	55	2
<i>p133</i>	SPU_015404	DN585544	55	1
<i>p16</i>	SPU_018408	DN784988	55	0.2
<i>p16rel1</i>	SPU_018403	DN578239	55	1
<i>p16rel2</i>	SPU_018407	DN561168	50	1
<i>p19</i>	SPU_004136	BG782044	55	0.5
<i>p41</i>	SPU_014065/019344	DN576989	55	2
<i>p58A</i>	SPU_000439	DN576150	60	0.5
<i>pks2</i>	SPU_028395	DN585039	55	1
<i>sfk3</i>	SPU_005419	DN806881	50	1
<i>sm20</i>	SPU_005991	DN562235	55	1.5
<i>sm27</i>	SPU_028945	DN578367	55	0.5
<i>sm29</i>	SPU_005990	DN576192	55	1
<i>sm30A</i>	SPU_000825	DN572785	60	0.5
<i>sm37</i>	SPU_018813	DN787584	60	0.5
<i>sm49</i>	SPU_027906	DN791580	55	1
<i>sm50</i>	SPU_018810/018811	DN785913	65	0.1
<i>SPU_027993</i>	SPU_027993	BG782104	55	1

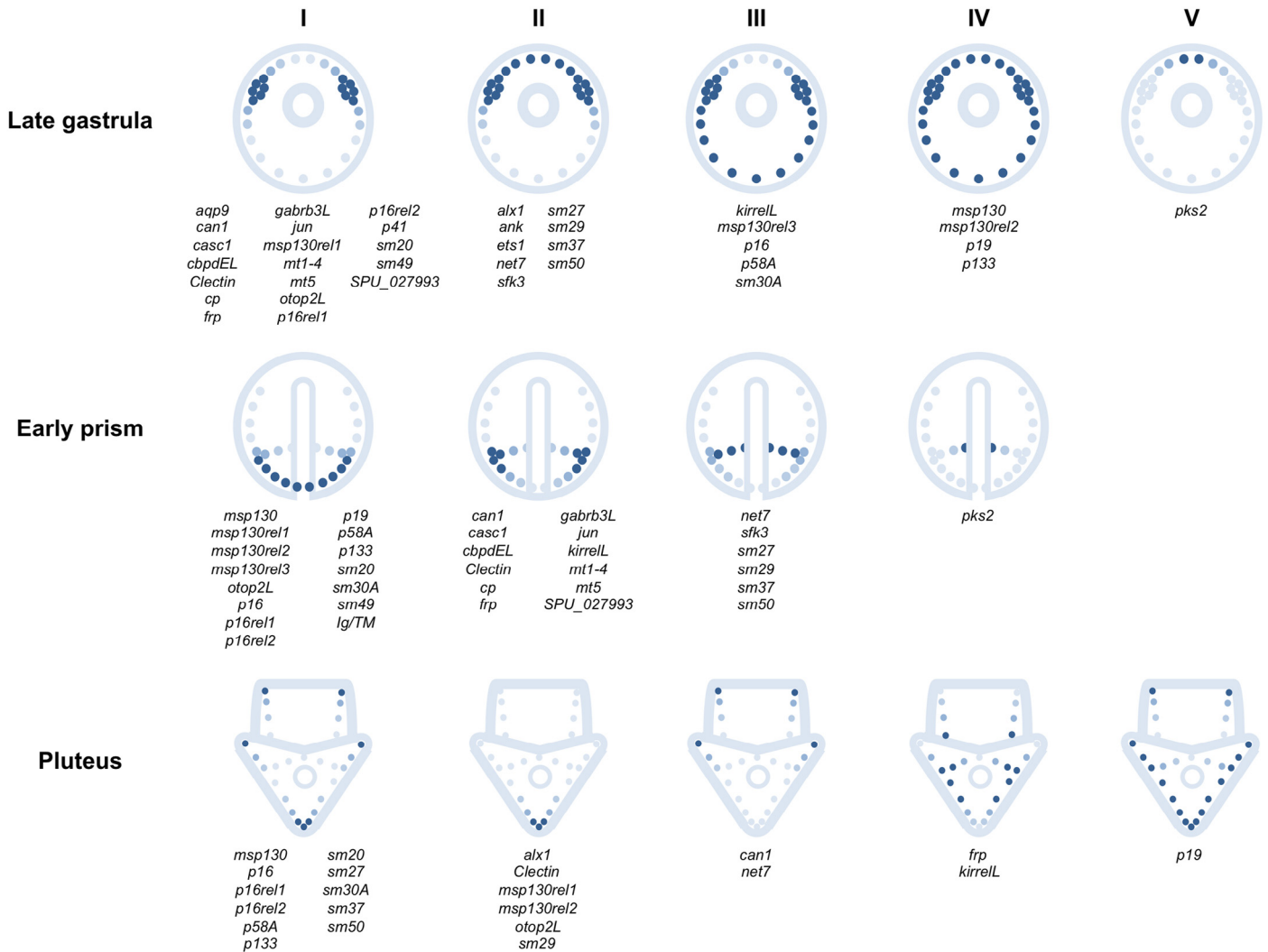


Fig. 2. Schematic diagrams illustrating spatial expression patterns of genes in the PMC GRN at the late gastrula (LG), early prism (EP), and pluteus (PL) stages (32, 48, and 76 hpf, respectively, at 15 °C). LG and PL embryos are shown viewed from the blastopore, and EP embryos are shown viewed from the ventral side. Five different expression categories were identified in LG embryos: Class I, higher expression level in the VLCs; Class II, higher expression level in the ventral chain and the VLCs; Class III, higher expression level in the dorsal chain and the VLCs; Class IV, uniform expression in all PMCs (this pattern was verified by titrating down these probes to ensure that this was not an artifact of very high expression and non-linear signal); Class V, higher expression level in the ventral chain. Four different expression patterns were detected in EP embryos: Class I, higher expression level in the dorsal chain and VLCs; Class II, higher expression level in the VLCs; Class III, higher expression level in the ventral chain and VLCs; Class IV, higher expression level in the ventral chain. Five different expression patterns were detected in PL embryos: Class I, higher expression level at the tips of the anterolateral, postoral and body rods; Class II, higher expression level at the tips of the body rods; Class III, higher expression level at the tips of the anterolateral and the postoral rods; Class IV, higher expression level in the PMCs that are relatively close to the original positions of the VLCs; Class V, higher expression level in all the PMCs that produce the body rods and the postoral rods and the PMCs at the tips of the anterolateral rods. mRNAs that could not be detected by WMISH at late stages are not listed. All diagrams show vegetal view of embryos.

msp130 and *msp130rel1* are members of the same protein family but had very different expression patterns at this stage. One general feature of the expression patterns at the late gastrula stage is that almost all genes (with the exception of *pks2*) were expressed at high levels in the VLCs, where the triradiate skeletal primordia form, in close association with patches of overlying ectoderm cells that express VEGF3 (Adomako-Ankomah and Etensohn, 2013; Duloquin et al., 2007).

At the early prism stage, the expression of 34 genes was detectable by WMISH and the expression patterns of these genes were classified into four categories. Fifteen genes were expressed at maximal levels in the dorsal chain and VLCs (Fig. 4, Class I); 12 genes were expressed only in the VLCs (Fig. 4, Class II); 6 genes were expressed at the highest level in the ventral chain and the VLCs (Fig. 4, Class III); and 1 gene (*pks2*) was expressed only in the ventral chain (Fig. 4, Class IV). All four genes that appeared to be uniformly

expressed in the PMC ring at the late gastrula stage (*msp130*, *msp130rel2*, *p19*, and *p133*) were differentially expressed in the dorsal chain and the VLCs (Class I) at the prism stage. Six genes (*msp130rel1*, *otop2L*, *p16rel1*, *p16rel2*, *sm20*, and *sm49*) that were expressed only in the VLCs at the earlier stage were also expressed in the dorsal chain at the prism stage (Class I). These observations suggest that an unidentified signaling pathway on the dorsal side of the embryo activates the expression of several genes in this region, where the body rods and later the schein form. Genes that showed Class II expression patterns at the late gastrula stage were still preferentially expressed in the PMCs at the same location at the early prism stage. The expression of *pks2* continued to be restricted to 2–3 PMCs in the ventral chain. The ventral transverse rods, which are produced by PMCs in the ventral chain, are the only skeletal rods that do not continue to elongate after gastrulation. It is possible that *pks2* (or other, unidentified genes with ventral-specific expression) might

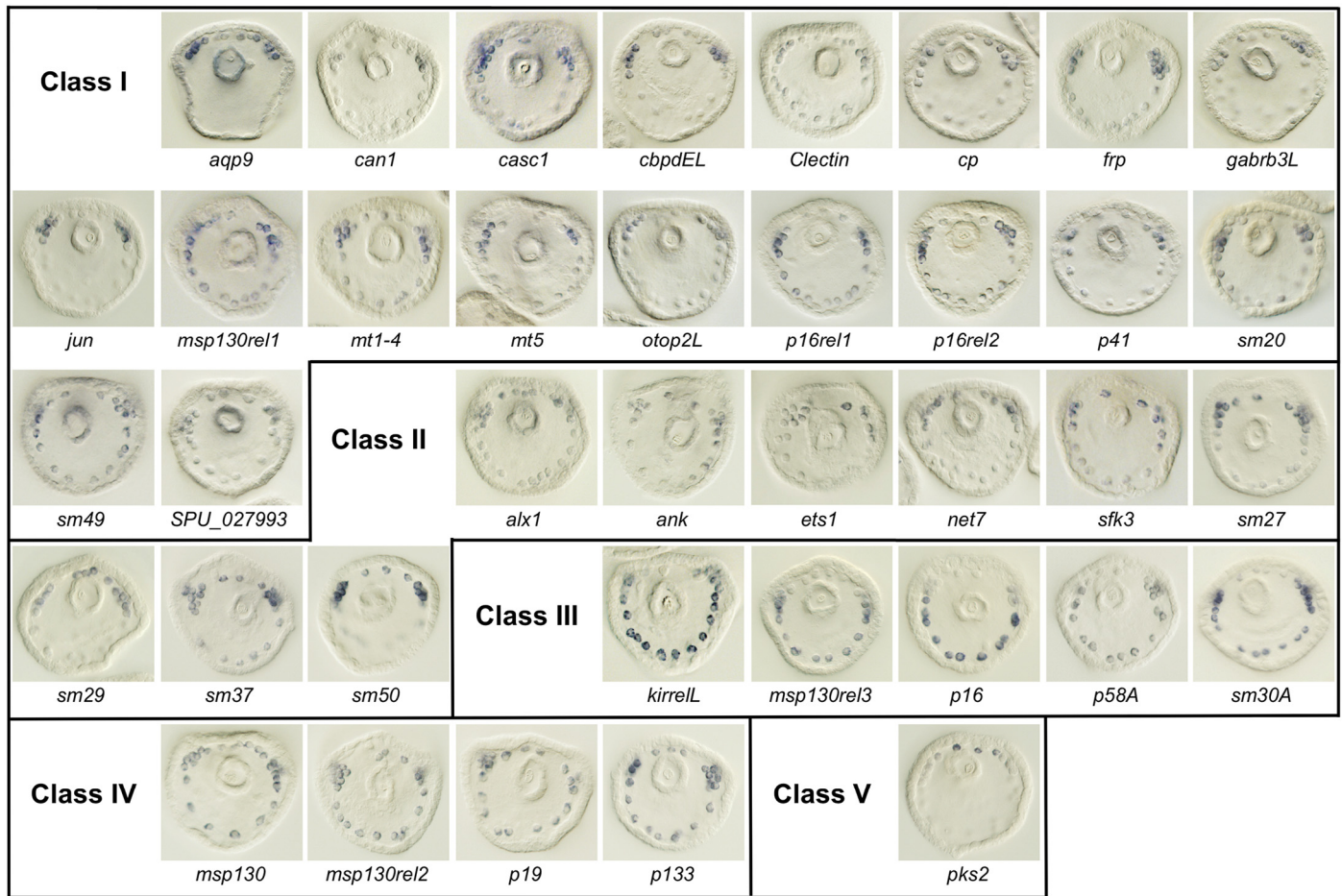


Fig. 3. Different expression patterns of PMC-specific/enriched mRNAs at the late gastrula stage. These mRNAs were classified into five groups based on their spatial expression patterns, as described in the legend to Fig. 1. All figures show vegetal view of embryos.

play a role in terminating the growth of the ventral transverse rods; alternatively, the general lack of expression of many biomineralization genes in the ventral chain may arrest the growth of these rods.

At the early prism stage, several genes were also asymmetrically expressed in the longitudinal chain of PMCs that extended from each VLC toward the animal pole (Fig. 5A). These PMCs produce the dorsoventral connecting rods, which in *S. purpuratus* curve ventrally, forming the anterolateral rods. Eleven genes were expressed at high levels in a very small number of PMCs (1–2 cells) at the tip of each longitudinal chain, near the animal pole (Fig. 5B). This observation suggests that a local signal in the animal ectoderm overlying the tips of the longitudinal chains activates gene expression in the neighboring PMCs. At the pluteus stage, only five of these mRNAs (*msp130*, *p16*, *p16rel1*, *p58A*, and *sm20*) were still detectable by WMISH. These transcripts were highly expressed at the tips of the anterolateral rods, which was consistent with their earlier expression patterns.

At the pluteus stage, the expression of 22 genes was detectable by WMISH and the expression patterns of these genes were classified into five categories. Eleven genes were expressed at higher levels at the tips of the body rods, the postoral rods and the anterolateral rods (Fig. 6, Class I). The expression of these genes may be regulated by both dorsal and the ventral ectodermal signals. Six genes were expressed only at the tips of the body rods (Fig. 6, Class II). These genes are likely to be regulated only by the dorsal signal. *can1* and *net7* were expressed at higher levels at the tips of the postoral rods and the anterolateral rods, but these mRNAs were not detected (or detected only at very low levels)

at the tips of the body rods (Fig. 6, Class III). *frp* and *kirreIL* were not expressed at a high level at the tips of any skeletal rods, but rather was maximally expressed in PMCs that were positioned relatively close to the original positions of the VLCs (Fig. 6, Class IV). Among the transcripts which were detectable by WMISH at all three stages, *can1*, *frp*, and *net7* are the ones which were not expressed dorsally. *p19* was expressed at a higher level in all the PMCs that give rise to the body rods and the postoral rods and the PMCs at the tips of the anterolateral rods (Fig. 6, Class V).

Several genes showed changes in their patterns of expression at the pluteus stage. One major trend was that the expression of several genes was activated in the dorsal region. For example, *sm27*, *sm29*, *sm37*, and *sm50* were not expressed at detectable levels by dorsal PMCs at the early prism stage (Class III), but were expressed by these cells at the pluteus stage (Classes I and II). Similarly, the expression of *Clectin* switched from the VLCs (Class II, early prism) to the dorsal PMCs (Class II, pluteus). Thus, in contrast to several other genes discussed above (*msp130rel1*, *otop2L*, *p16rel1*, *p16rel2*, *sm20*, and *sm49*), these five genes (*sm27*, *sm29*, *sm37*, *sm50*, and *Clectin*) were not expressed by dorsal PMCs until the pluteus stage.

1.2. Regulation of PMC gene expression by the VEGF and MAPK pathways

We asked whether the non-uniform patterns of gene expression we observed might be dependent upon VEGF and/or MAPK signaling. To address this question, we examined the effects of

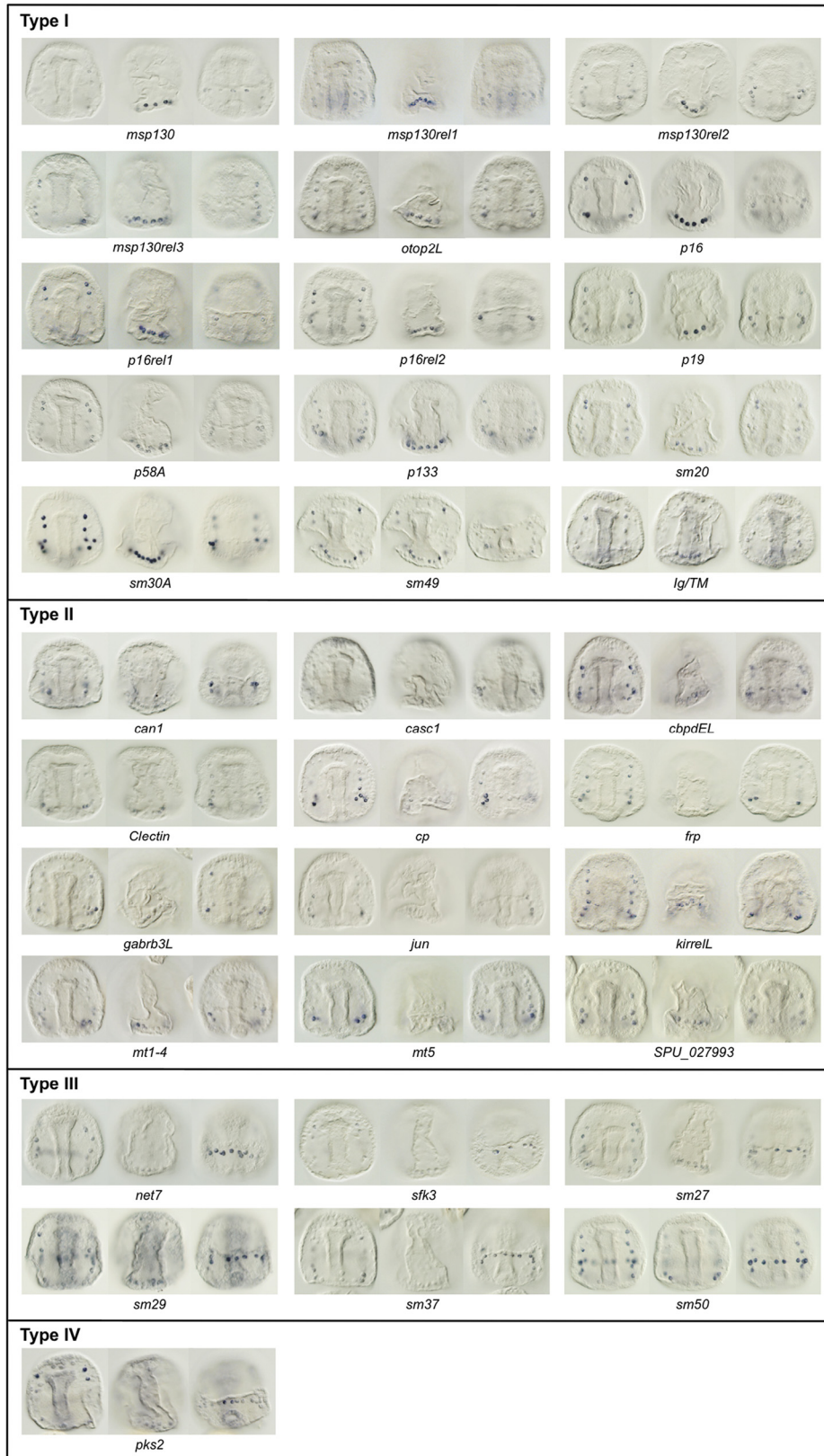


Fig. 4. Different expression patterns of PMC-specific/enriched mRNAs at the early prism stage. These mRNAs were classified into four groups based on their spatial expression patterns, as described in the legend to Fig. 2. Two to three focal planes of an embryo are shown for each mRNA.

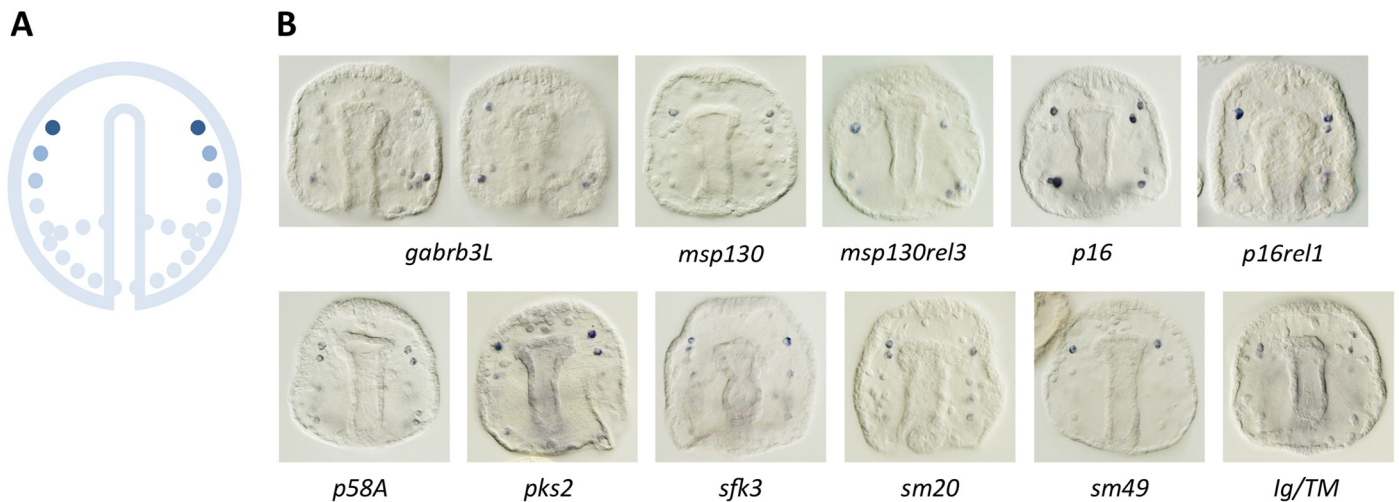


Fig. 5. WMISH analysis of gene expression in the PMCs at the tips of the longitudinal chains at the early prism stage. (A) A schematic diagram illustrating elevated mRNA expression levels in a small number of PMCs at the tips of the longitudinal chains that extend from the VLCs toward the animal pole. (B) WMISH analysis of genes that are expressed at a higher level in the PMCs at the tips of the longitudinal chains.

axitinib, a selective VEGFR inhibitor (Adomako-Ankomah and Etensohn, 2013) and U0126, a MEK inhibitor, on the expression patterns of genes that showed Class I, III, and V expression patterns in control plutei (Fig. 7). To circumvent the early effects of these drugs on PMC specification and migration, embryos were treated at the early prism stage, after the PMC pattern was well established. Inhibitor-treated and control embryos were fixed at the pluteus stage, after 24 hr of continuous exposure to the inhibitors, and analyzed by WMISH. Eleven out of 13 genes tested were down-regulated in PMCs at the tips of the anterolateral and postoral rods in both axitinib and U0126-treated embryos (Fig. 7A). These results indicate that VEGF- and MEK-mediated signaling is required for the local expression of genes at the tips of these rods, which extend from the ventral surface of the embryo. The two exceptions we observed were the following: a) in U0126-treated embryos, *p16rel1* was down-regulated only at the tips of the postoral rods but not the anterolateral rods (in contrast, axitinib treatment caused a loss of *p16rel1* expression at the tips of both rods); b) both inhibitors caused a reduction in *p19* mRNA levels at the tips of the anterolateral rods, but did not noticeably affect expression at the tips of the postoral rods (Fig. 7B).

The same suite of genes (with the exception of *can1*) was also highly expressed at the tips of the body rods in control embryos. In contrast to the effects of axitinib and U0126 on gene expression at the tips of the anterolateral and postoral rods, these inhibitors did not have a detectable effect on gene expression at the tips of the body rods (Fig. 7). This finding strongly supports the view that gene expression in the dorsal region is regulated by a signal distinct from VEGF.

2. Discussion

Our observations show that many effector genes and at least some regulatory genes shift from a cell-autonomous to a signal-dependent mode during gastrulation. One important effect of this global shift in regulatory mechanisms is to maintain high levels of skeletogenic mRNAs in specific subpopulations of PMCs, while levels decline in other cells in the syncytium. The transition from ubiquitous to restricted gene expression within the PMC population accounts for the fact that, when measured on a per-embryo basis, the levels of many effector mRNAs decline during post-gastrula stages of

development, when overt skeleton deposition takes place (Rafiq et al., 2014).

Sites of elevated mRNA expression within the PMC syncytium likely reflect sites where rates of transcription are relatively high. Alternately, the accumulation of mRNAs at specific locations within the PMC syncytial network might result from the diffusion and selective trapping of mRNAs, directional mRNA transport, or localized stabilization of transcripts. Although definitive evidence is lacking, long-range diffusion of mRNAs within the PMC syncytium does not appear to occur, based on the observation that transcripts produced from transgenes driven by PMC-specific promoters remain localized near the site of synthesis (Harkey et al., 1995; Wilt et al., 2008). Whatever the mechanism that generates non-uniform distributions of mRNAs, once these are established, stable protein asymmetries can be maintained within the PMC syncytium. Immunostaining using antibodies against SM30, SM50, PM27/SM27, and Tbx2/3 shows that the spatial distributions of these proteins are similar to those of the corresponding mRNAs (Gross et al., 2003; Harkey et al., 1995; Urry et al., 2000).

What controls the temporal and spatial pattern of spiculogenesis? Many biomineralization-related mRNAs (and proteins) are expressed maximally prior to gastrulation (Harkey and Whiteley, 1983; Rafiq et al., 2014), yet spicules do not form until much later in development. One hypothesis is that overt skeletogenesis is delayed until PMC fusion has taken place, as fusion might be required in order to create an appropriate intracellular compartment for biomineral assembly. PMC fusion cannot fully account for the spatial or temporal pattern of skeletogenesis, however, for several reasons: 1) fusion occurs well in advance of spicule formation (Hodor and Etensohn, 1998); 2) cultured micromeres fuse when cultured in the absence of serum, yet spicules do not form under these conditions, indicating that additional signals are required; 3) when spiculogenesis begins *in vivo*, all PMCs have undergone fusion and are joined in a single syncytial network, yet spicule rudiments arise only within the VLCs. Thus, although PMC fusion may be required for skeletogenesis, other regulatory mechanisms must be invoked to explain the temporal and spatial patterns of skeletal growth observed *in vivo*. An alternative hypothesis, which we favor, is that one or more essential effectors of biomineralization are not expressed during the early, cell-autonomous regulatory phase (or are expressed at levels too low to support overt spiculogenesis), and these

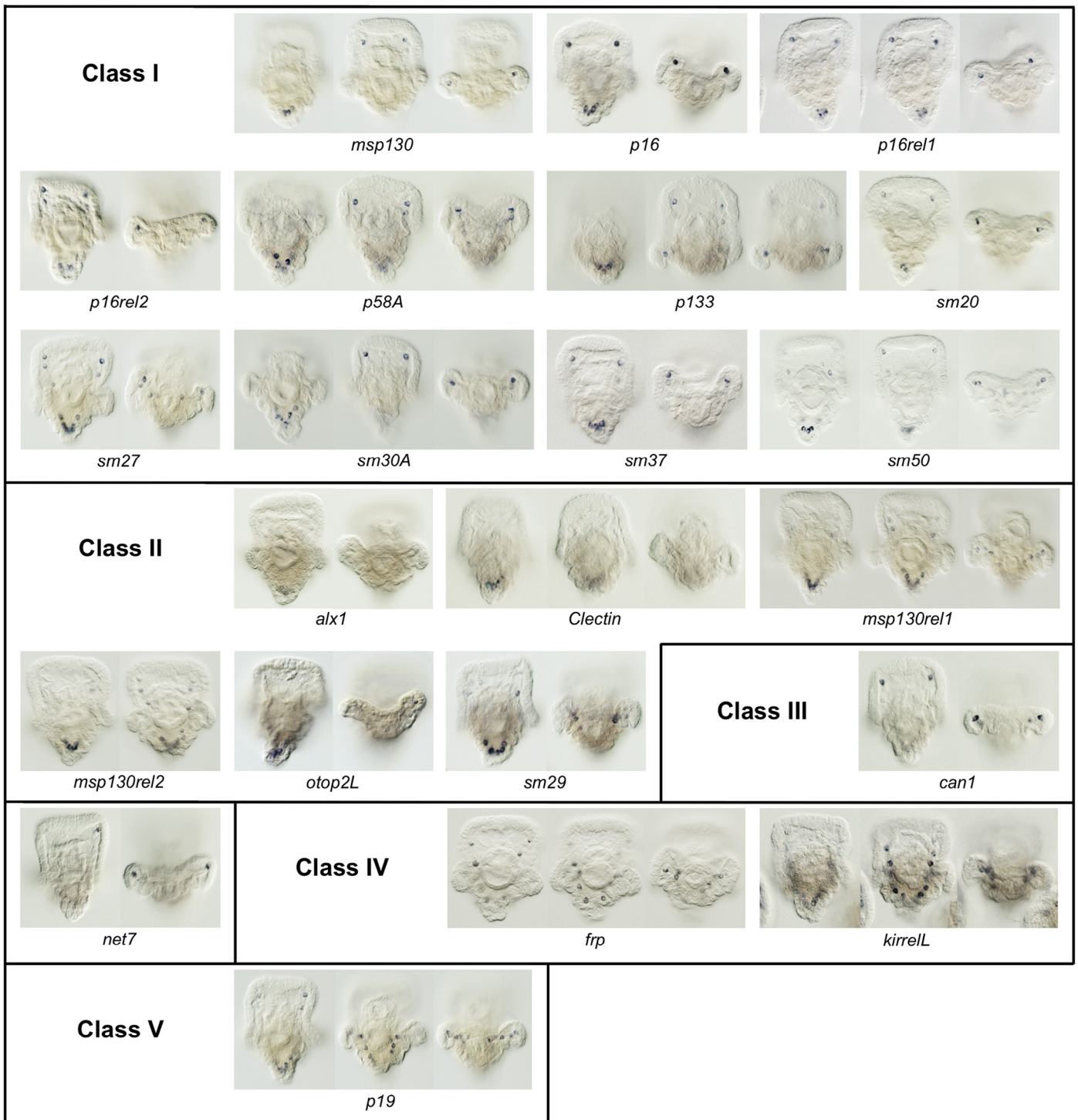


Fig. 6. WMISH analysis of PMC-specific/enriched mRNAs at the pluteus stage. These mRNAs were classified into five groups based on their spatial expression patterns, as described in the legend to Fig. 2. Two to three focal planes of an embryo are shown for each mRNA.

genes are activated only during the late, signal-dependent phase of regulation. This model is consistent with the observation that although most effector mRNAs are expressed at high levels during the early, cell-autonomous phase of development, some accumulate only later in development (Rafiq et al., 2014).

Our studies show that multiple signals influence PMC gene expression and skeletal growth (note that here we are primarily concerned with signals that act directly on PMCs, rather than signals that act earlier in development to pattern the ectoderm). VEGF3 is

expressed by patches of ectoderm cells located at the tips of the anterolateral and postoral rods, skeletal elements that extend from the ventral surface of the embryo and support the first pairs of larval arms (Adomako-Ankomah and Ettensohn, 2013; Duloquin et al., 2007). Adomako-Ankomah and Ettensohn (2013) showed that inhibition of VEGF signaling during post-gastrula development resulted in a selective inhibition of the growth of the anterolateral and postoral rods. Here, we extend these observations by demonstrating that VEGF signaling is required to maintain the localized expression of

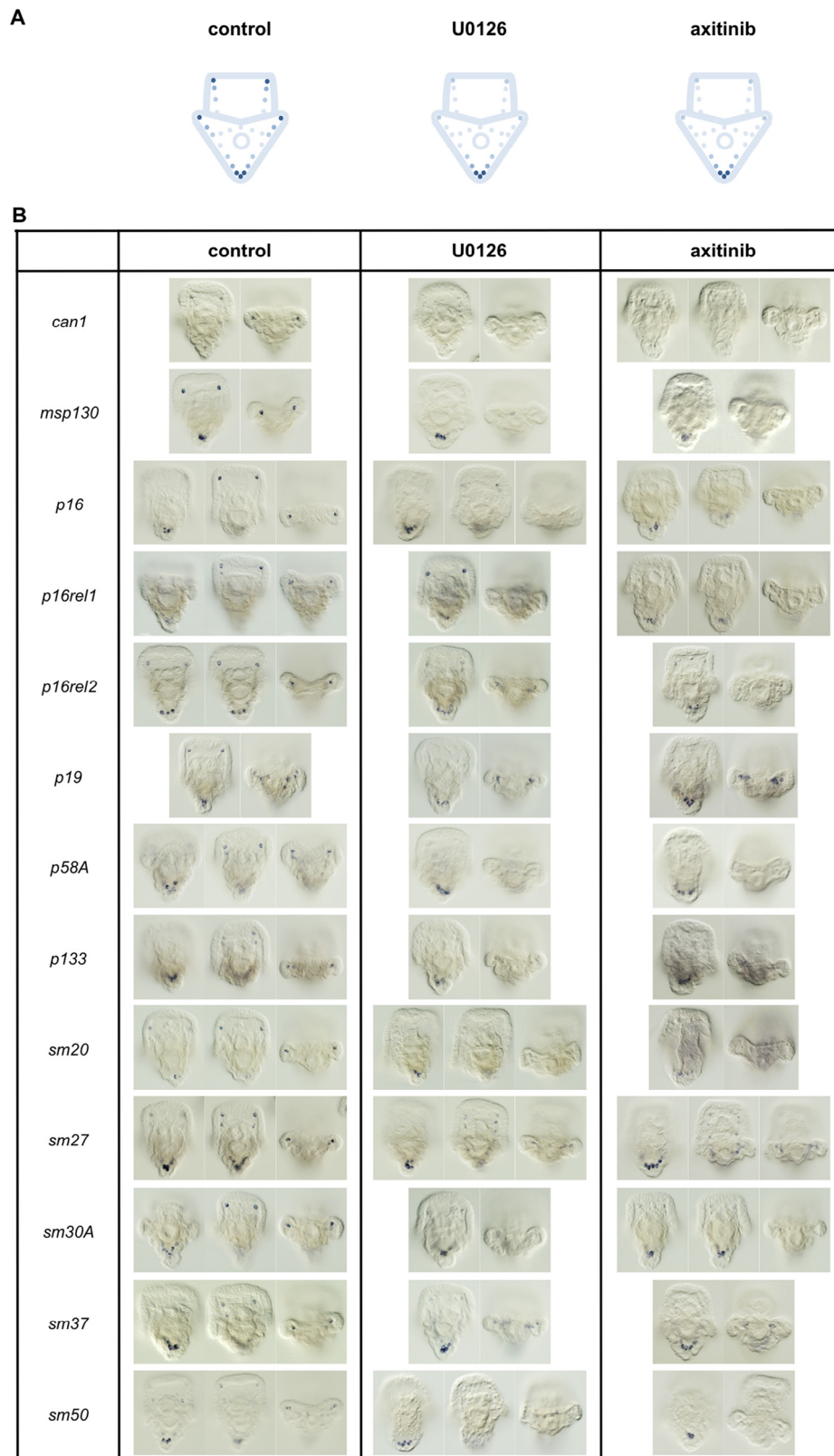


Fig. 7. The MAPK and VEGF pathways are required for the elevated expression of effector mRNAs in PMCs at the tips of the postoral rods and the anterolateral rods. (A) Diagram showing the effect of U0126 and axitinib on gene expression by PMCs at the tips of postoral rods and anterolateral rods. (B) WMISH analysis of gene expression in control, U0126-treated, and axitinib-treated embryos. The genes shown are expressed at higher levels in the PMCs at the tips of postoral rods and anterolateral rods (Classes I, III and V, pluteus stage). All transcripts are downregulated at the tips of both the postoral rods and the anterolateral rods in U0126- and axitinib-treated embryos except *p19* (unaffected at the tips of the postoral rods in both treatments) and *p16rel1* (unaffected at the tips of the anterolateral rods in U0126-treated embryos).

effector genes in PMCs at the tips of these rods. Our findings confirm that VEGF acts as a key regulator of skeletogenesis, independent of its role in directing PMCs to the appropriate target sites on the blastocoel wall.

Most effector mRNAs are expressed preferentially in the VLCs during gastrulation and at much lower (or, in some cases, undetectable) levels in the dorsal region. At post-gastrula stages, however, many of these same mRNAs, in addition to their ventral expression, begin to accumulate dorsally, eventually accumulating to high levels at the posterior apex of the larva, where the scheidel will form. Other recent studies have also documented elevated expression of mRNAs in the dorsal region at post-gastrula stages (Luo and Su, 2012; Solek et al., 2013). VEGF3 is not expressed dorsally and the expression of genes in this region of the PMC syncytium is unaffected by axitinib; these findings indicate that a different signaling pathway functions in this region. We noted some asynchrony among effector genes with respect to the activation of dorsal expression; this might indicate that some effector genes are regulated more directly by the dorsal signal than others, or that more than one signal acts dorsally. One candidate for a late, dorsal signal is BMP2/4, which is known to function on this side of the embryo throughout much of embryogenesis (Molina et al., 2013). Direct evidence of a localized activation of BMP signaling in dorsal PMCs comes from the specific accumulation of active (phosphorylated) SMAD1/5/8 in their nuclei (Lapraz et al., 2009). Our preliminary studies using various BMP signaling inhibitors, however, have not provided clear-cut support for the hypothesis that BMP signaling regulates gene expression or skeletal growth on the dorsal side of the embryo during late embryogenesis (Sun and Etensohn, unpublished observations).

It is widely believed that micromeres and an early-ingressing skeletogenic mesenchyme are relatively recent evolutionary inventions among the echinoderms (Etensohn, 2013; Gao and Davidson, 2008). Thus, the cell-autonomous phase of the regulation of the skeletogenic GRN is also likely to be derived, and the later, signal-dependent phase of GRN regulation may more closely resemble the ancestral program of skeletogenic specification in the phylum. This program likely underwent repeated heterochronic shifts during echinoid evolution (Etensohn, 2009, 2013), but features of the ancestral program may be gleaned from studies on skeletogenic specification in echinoderms that lack micromeres and form skeletal elements much later in development, such as cidaroid sea urchins (Yamazaki et al., 2012) and sea stars (Morino et al., 2012).

3. Experimental procedures

3.1. Embryo culture

Adult *S. purpuratus* were obtained from Pat Leahy (California Institute of Technology, Pasadena, CA, USA). Gametes were obtained by intracoelomic injection of 0.5 M KCl and embryos were cultured in artificial seawater (ASW) at 15 °C.

3.2. Inhibitor treatments

Five millimolar stock solutions of U0126 (EMD Millipore, Catalog #662005) and axitinib (Selleckchem, Catalog #S1005) were prepared in dimethylsulfoxide (DMSO) and aliquots were stored at -20 °C. Working dilutions were prepared in ASW immediately before use and added to embryos at the early prism stage, 48 hours post-fertilization (hpf) at final concentrations of 7 μM (U0126) or 50 nM (axitinib). Sibling control embryos were cultured in equivalent concentrations of DMSO. Inhibitor-treated and control embryos were fixed for WMISH at the pluteus stage (72 hpf).

3.3. Whole mount in situ hybridization (WMISH)

Embryos were fixed for 1 hr at room temperature in 4% paraformaldehyde in ASW and stored in 100% methanol at 4 °C. WMISH was performed as described previously (Duloquin et al., 2007). Probes derived from pSPORT vectors were synthesized using clones from an *S. purpuratus* PMC cDNA library as templates (Rafiq et al., 2012). Incubation temperatures and the final concentration of each probe are shown in Table 1.

Acknowledgement

This work was supported by National Science Foundation Grant IOS-1021805 to C.A.E.

References

- Adomako-Ankomah, A., Etensohn, C.A., 2011. P58-A and P58-B: novel proteins that mediate skeletogenesis in the sea urchin embryo. *Dev. Biol.* 353 (1), 81–93.
- Adomako-Ankomah, A., Etensohn, C.A., 2013. Growth factor-mediated mesodermal cell guidance and skeletogenesis during sea urchin gastrulation. *Development* 140 (20), 4214–4225.
- Armstrong, N., Hardin, J., McClay, D.R., 1993. Cell-cell interactions regulate skeleton formation in the sea urchin embryo. *Development* 119 (3), 833–840.
- Beeble, A., Calestani, C., 2012. Expression pattern of *polyketide synthase-2* during sea urchin development. *Gene Expr. Patterns* 12 (1), 7–10.
- Cheers, M.S., Etensohn, C.A., 2005. P16 is an essential regulator of skeletogenesis in the sea urchin embryo. *Dev. Biol.* 283 (2), 384–396.
- Duloquin, L., Lhomond, G., Gache, C., 2007. Localized VEGF signaling from ectoderm to mesenchyme cells controls morphogenesis of the sea urchin embryo skeleton. *Development* 134 (12), 2293–2302.
- Etensohn, C.A., 2009. Lessons from a gene regulatory network: echinoderm skeletogenesis provides insights into evolution, plasticity and morphogenesis. *Development* 136 (1), 11–21.
- Etensohn, C.A., 2013. Encoding anatomy: developmental gene regulatory networks and morphogenesis. *Genesis* 51 (6), 383–409.
- Etensohn, C.A., Malinda, K.M., 1993. Size regulation and morphogenesis: a cellular analysis of skeletogenesis in the sea urchin embryo. *Development* 119 (1), 155–167.
- Fernandez-Serra, M., Consales, C., Livigni, A., Arnone, M.I., 2004. Role of the ERK-mediated signaling pathway in mesenchyme formation and differentiation in the sea urchin embryo. *Dev. Biol.* 268 (2), 384–402.
- Gao, F., Davidson, E.H., 2008. Transfer of a large gene regulatory apparatus to a new developmental address in echinoid evolution. *Proc. Natl Acad. Sci. U.S.A.* 105 (16), 6091–6096.
- Gross, J.M., Peterson, R.E., Wu, S.Y., McClay, D.R., 2003. LvTbx2/3: a T-box family transcription factor involved in formation of the oral/aboral axis of the sea urchin embryo. *Development* 130 (9), 1989–1999.
- Guss, K.A., Etensohn, C.A., 1997. Skeletal morphogenesis in the sea urchin embryo: regulation of primary mesenchyme gene expression and skeletal rod growth by ectoderm-derived cues. *Development* 124 (10), 1899–1908.
- Hardin, J., Coffman, J.A., Black, S.D., McClay, D.R., 1992. Commitment along the dorsoventral axis of the sea urchin embryo is altered in response to NiCl₂. *Development* 116 (3), 671–685.
- Harkey, M.A., Whiteley, A.H., 1983. The program of protein synthesis during the development of the micromere-primary mesenchyme cell line in the sea urchin embryo. *Dev. Biol.* 100 (1), 12–28.
- Harkey, M.A., Whiteley, H.R., Whiteley, A.H., 1992. Differential expression of the *msp130* gene among skeletal lineage cells in the sea urchin embryo: a three dimensional in situ hybridization analysis. *Mech. Dev.* 37 (3), 173–184.
- Harkey, M.A., Klueg, K., Sheppard, P., Raff, R.A., 1995. Structure, expression, and extracellular targeting of PM27, a skeletal protein associated specifically with growth of the sea urchin larval spicule. *Dev. Biol.* 168 (2), 549–566.
- Hodor, P.G., Etensohn, C.A., 1998. The dynamics and regulation of mesenchymal cell fusion in the sea urchin embryo. *Dev. Biol.* 199 (1), 111–124.
- Illies, M.R., Peeler, M.T., Dechtiaruk, A.M., Etensohn, C.A., 2002. Identification and developmental expression of new biomineralization proteins in the sea urchin *Strongylocentrotus purpuratus*. *Dev. Genes Evol.* 212 (9), 419–431.
- Knapp, R.T., Wu, C.H., Mobilia, K.C., Joester, D., 2012. Recombinant sea urchin vascular endothelial growth factor directs single-crystal growth and branching in vitro. *J. Am. Chem. Soc.* 134 (43), 17908–17911.
- Lapraz, F., Besnardeau, L., Lepage, T., 2009. Patterning of the dorsal-ventral axis in echinoderms: insights into the evolution of the BMP-chordin signaling network. *PLoS Biol.* 7 (11), e1000248.
- Li, E., Materna, S.C., Davidson, E.H., 2013. New regulatory circuit controlling spatial and temporal gene expression in the sea urchin embryo oral ectoderm GRN. *Dev. Biol.* 382 (1), 268–279.
- Li, E., Cui, M., Peter, I.S., Davidson, E.H., 2014. Encoding regulatory state boundaries in the pregastrular oral ectoderm of the sea urchin embryo. *Proc. Natl Acad. Sci. U.S.A.* 111 (10), E906–E913.

- Livingston, B.T., Killian, C.E., Wilt, F., Cameron, A., Landrum, M.J., Ermolaeva, O., et al., 2006. A genome-wide analysis of biomineralization-related proteins in the sea urchin *Strongylocentrotus purpuratus*. *Dev. Biol.* 300 (1), 335–348.
- Luo, Y.J., Su, Y.H., 2012. Opposing nodal and BMP signals regulate left–right asymmetry in the sea urchin larva. *PLoS Biol.* 10 (10), e1001402.
- McCarthy, R.A., Spiegel, M., 1983. Serum effects on the in vitro differentiation of sea urchin micromeres. *Exp. Cell Res.* 149 (2), 433–441.
- McIntyre, D.C., Seay, N.W., Croce, J.C., McClay, D.R., 2013. Short-range Wnt5 signaling initiates specification of sea urchin posterior ectoderm. *Development* 140 (24), 4881–4889.
- McIntyre, D.C., Lyons, D.C., Martik, M., McClay, D.R., 2014. Branching out: origins of the sea urchin larval skeleton in development and evolution. *Genesis* 52 (3), 173–185.
- Molina, M.D., de Crozé, N., Haillet, E., Lepage, T., 2013. Nodal: master and commander of the dorsal–ventral and left–right axes in the sea urchin embryo. *Curr. Opin. Genet. Dev.* 23 (4), 445–453.
- Morino, Y., Koga, H., Tachibana, K., Shoguchi, E., Kiyomoto, M., Wada, H., 2012. Heterochronic activation of VEGF signaling and the evolution of the skeleton in echinoderm pluteus larvae. *Evol. Dev.* 14 (5), 428–436.
- Okazaki, K., 1975. Spicule formation by isolated micromeres of the sea urchin embryo. *Am. Zool.* 15 (3), 567–581.
- Oliveri, P., Tu, Q., Davidson, E.H., 2008. Global regulatory logic for specification of an embryonic cell lineage. *Proc. Natl Acad. Sci. U.S.A.* 105 (16), 5955–5962.
- Page, L., Benson, S., 1992. Analysis of competence in cultured sea urchin micromeres. *Exp. Cell Res.* 203 (2), 305–311.
- Rafiq, K., Cheers, M.S., Etensohn, C.A., 2012. The genomic regulatory control of skeletal morphogenesis in the sea urchin. *Development* 139 (3), 579–590.
- Rafiq, K., Shashikant, T., McManus, C.J., Etensohn, C.A., 2014. Genome-wide analysis of the skeletogenic gene regulatory network of sea urchins. *Development* 141 (4), 950–961.
- Röttinger, E., Besnardeau, L., Lepage, T., 2004. A Raf/MEK/ERK signaling pathway is required for development of the sea urchin embryo micromere lineage through phosphorylation of the transcription factor Ets. *Development* 131 (5), 1075–1087.
- Schlessinger, J., 2000. Cell signaling by receptor tyrosine kinases. *Cell* 103 (2), 211–225.
- Sharma, T., Etensohn, C.A., 2010. Activation of the skeletogenic gene regulatory network in the early sea urchin embryo. *Development* 137 (7), 1149–1157.
- Solek, C.M., Oliveri, P., Loza-Coll, M., Schrankel, C.S., Ho, E.C.H., Wang, G., et al., 2013. An ancient role for Gata-1/2/3 and Scl transcription factor homologs in the development of immunocytes. *Dev. Biol.* 382 (1), 280–292.
- Stephens, L., Kitajima, T., Wilt, F., 1989. Autonomous expression of tissue-specific genes in dissociated sea urchin embryos. *Development* 107 (2), 299–307.
- Urry, L.A., Hamilton, P.C., Killian, C.E., Wilt, F.H., 2000. Expression of spicule matrix proteins in the sea urchin embryo during normal and experimentally altered spiculogenesis. *Dev. Biol.* 225 (1), 201–213.
- Wilt, F.H., Etensohn, C.A., 2007. The morphogenesis and biomineralization of the sea urchin larval skeleton. *Handbook of Biomineralization: Biological Aspects and Structure Formation*, 182–210.
- Wilt, F.H., Killian, C.E., Hamilton, P., Croker, L., 2008. The dynamics of secretion during sea urchin embryonic skeleton formation. *Exp. Cell Res.* 314 (8), 1744–1752.
- Yamazaki, A., Kidachi, Y., Minokawa, T., 2012. Micromere” formation and expression of endomesoderm regulatory genes during embryogenesis of the primitive echinoid *Prionocidaris baculosa*. *Dev. Growth Differ.* 54 (5), 566–578.